경사가로줄눈을 가진 콘크리트포장구조의 유한요소법에 의한 해석

A Finite Element Analysis for the Concrete Highway Pavements with Skewd Joints

조 병 완*
Jo, Byung Wan

요 지

20세기에 들어서 포틀랜드 시멘트 콘크리트를 이용한 강성포장은, 콘크리트재료의 구조적인 휨강성과 큰 탄성계수 그리고 내구성을 고려한 경제성 등으로 세계 여러 나라에서 널리 이용되어져 왔다.

그러나, 완변한 설계 및 시공에도 불구하고, 일부 콘크리트 포장도로에서는(예 : 미국 Interstate-10 and 75, 한국의 88 고속도로 및 중부 고속도로) 심각한 종적, 횡적 균열 및 침하현상 등으로 보수, 유지의 큰 어려움을 겪고 있는 바, 이러한 문제점을 구조역학적인 입장에서 유한 요소법을 이용한 콘크리트 포장구조의 해석을 통해, 차량 위치 및 온도변화에 따른 최대 파괴응력과 위치, 그리고 최대 처짐 등을 고려 하므로써, 콘크리트 포장도로의 구조적인 문제점을 해결하는 데 있다.

본 논문에서는 요즘 미국에서 널리 이용되고 있는 경가가로줄눈(skewed joint)의 효과를 구조역학적으로 해석을 하였다.

Abstract

In twentieth century, a rigid pavement composed of a series of thin Portland Cement Concrete has been accepted due to the desirable structural strength of concrete, durability and economy.

However, despite of precise design and construction of concrete highway pavements, some of concrete pavements (example : Interstate-10 and 75 in U.S.A, 88 Olympic express highway and Jung-bu express highway in Korea) has already shown severe signs of longitudinal and transverse cracking, faulting, and pumping before the end of their intended service life. This highlights the need for better understanding of concrete pavement behavior using structural analysis program.

For these reasons, this research was performed to study an analytical behavior of concrete pavements, especially for the effects of skewed joints on concrete pavements. Subsequently, this research should give better understanding of concrete pavement behavior to the highway engineers and provide effective remedies to the concrete highway pavements.

*정회원 · 한남대학교 이공대학 조교수, 토목공학과

1. Introduction

This research was performed to study an analytical behavior of concrete highway pavements with skewed joints. In order to extend the capability of a previous finite element analysis program, an effort was undertaken to derive the stiffness matrix and equivalent nodal load matrices due to the temperature variations, frictional resistance and uniformly distributed loads on parallelogrammic plate bending elements.

The program, FEACONS(Finite Element Analysis of Concrete Slabs) originally developed at the Department of Civil Engineering, University of Florida, was expanded from a rectangular element to a parallelogrammic element to consider the skewed joint pavement system. This program FEACONS V[1] can analyze a three continuous slab system with the consideration of the effects of skewed joint, live load, dead load, subgrade voids, joint conditions and temperature variations within the concrete slab.

Using this program, a comparative study was performed to investigate the effects of skewed joints on concrete pavement system. Furthermore, a maximum principal stress profile was presented to show lines of constant principal stress on the surface of the slab. This provides a very concise way of looking at the distribution of stresses and helps highway engineers understand how they interact in the pavement system.

2. Parallelogrammic Plate Bending Element

The element used in this analysis is the four nodes parallelogrammic plate bending element as shown in Figure 1. The material that comprises the element is assumed to be linear elastic, homogeneous, and isotropic. This element has a vertical deflection w and

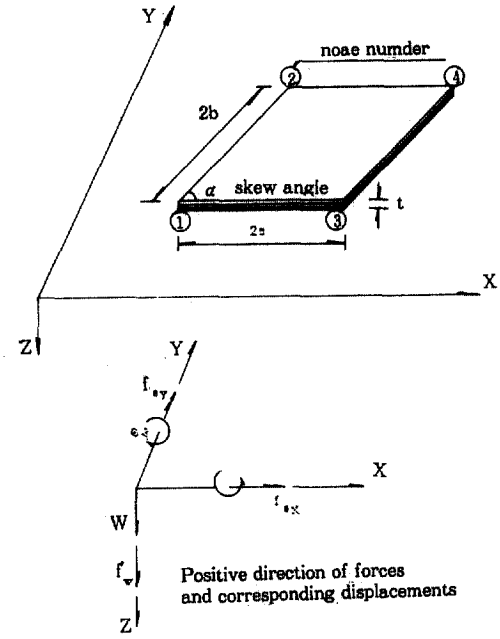

Fig. 1. Dimensions and Positive direction of a Parallelogram Plate Bending Element.

two rotations about x, y axis, for a total of twelve degrees of freedom per element.

The displacements shown in this figure correspond with the assumed positive directions of nodal forces at the each nodes. The array of nodal displacements is :

$$q_i = \begin{bmatrix} q_{i1} \\ q_{i2} \\ q_{i3} \end{bmatrix} = \begin{bmatrix} W_i \\ \theta_{xi} \\ \theta_{yi} \end{bmatrix} = \begin{bmatrix} W_i \\ -dw_i/dy \\ dw_i/dx \end{bmatrix}$$

(where, $i=1, 2, 3, 4$ node number)

The array of corresponding nodal forces is:

$$P_i = \begin{bmatrix} P_{i1} \\ P_{i2} \\ P_{i3} \end{bmatrix} = \begin{bmatrix} F_{zi} \\ M_{xi} \\ M_{yi} \end{bmatrix}$$

If we assume the generic displacement function, vertical displacement W, within an element expressed in terms of x, y coordinates is :

$$W = C_1 + C_2X + C_3Y + C_4X^2 + C_5XY + C_6Y^2 + C_7 \cdot X^3 + C_8 \cdot X^2Y + C_9X \cdot Y^2 + C_{10} \cdot Y^3 + C_{11}X^3 \cdot Y + C_{12} \cdot XY^3$$

which is a complete cubic of ten terms and

two quartic terms. From this assumption, it is possible to derive the displacemment shape functions, stiffness matrix, equivalent load matrices based on the displacement-strain-stress relationship and virtual work basis of finite element methods. For reference, the stiffness matrix of parallelogrammic plate bending element is given in appendix.

3. Computer Modeling

A jointed concrete pavement is modeled by a three continuous slab system with two intermediate joints as shown in Figure 2.[2] Each concrete slab is modeled as an assemblage of parallelogrammic plate bending elements.

Load transfers across the transverse joints between two adjoining slabs are modeled by shear (or linear) and rotational (or torsional) springs connecting the slabs at the nodes of the elements along the joint.

Frictional effects of the tie bars at the longitudinal joints are modeled by shear springs at the nodes along the longitudinal edges.

The subgrade is modeled as a Winkler foundation which is modeled by a series of vertical springs at the nodes. Subgrade voids are modeled as initial gaps between the slab and the springs at the nodes. A spring stiffness of zero is used when a gap exists.

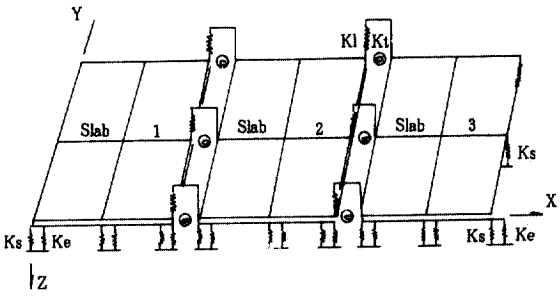

Fig. 2. Finite Element Modeling of a Three Slab Pavement System (Ref. 1).

4. Development of Analytical Tools

A computer program (FEACONS V) was developed by Jo, Byung-wan, Shau Lei[3], Kevin Lee Toye[4], at the Department of Civil Engineering, University of Florida. The simplified flow chart of this program is shown in Figure 3.

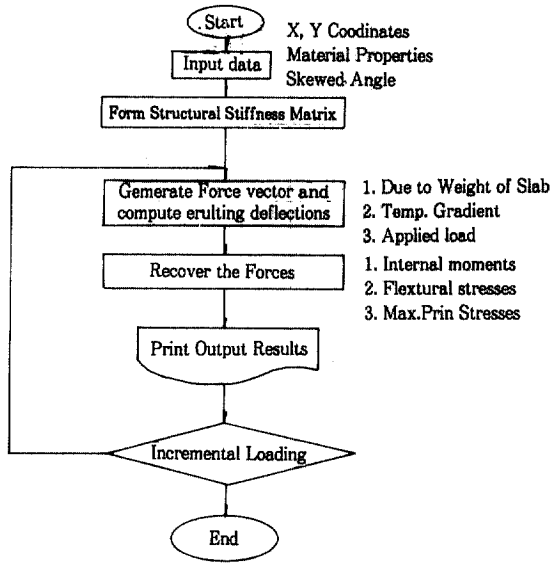

Fig. 3. Simplified Flow Chart of Feacons Ⅳ Program.

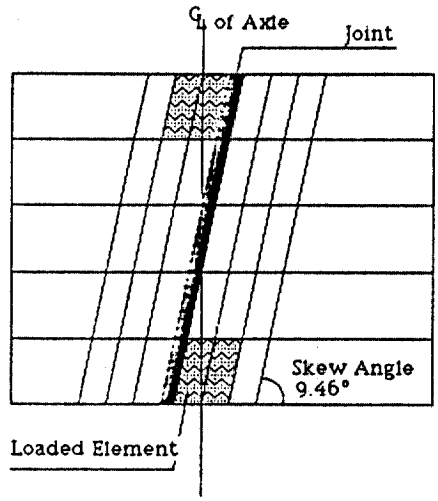

Fig. 4. Uniform Axie Load on Skewed Joint Element.

5. Case Study : Effects of Skewed Joints on Concrete Pavements

Case study was performed to investigate the effects of skewed joints on the structural response of concrete pavements. The design information and field data considered were those which were relevant to the Interstate-75 concrete pavement in Florida, U. S.A. (Refer to Figure 4.)

5. 1. Input data

Slab dimensions : Length = 22 ft(6.7 m),
Width = 12 ft(3.65 m),
Thickness = 9inch(22.9cm)

Skew angle : 0, 9.4623°, 18.4°

Material properties : Density of concrete = 140 pcf(2.24 t/m^3)
Elastic modulus of concrete = 5290 ksi (370000kg/cm^3)
Poisson's ratio of concrete = 0.2

Spring stiffness : Subgrade spring stiffness = 0.175 kci(4.85 kg/cm^3)
Rotational joint stiffness = 16,000 k/in (2860 t/cm)
Linear joint stiffness = 10 ksi (7000 kg/cm^2)
Edge spring stiffness = 10 ksi (7000 kg/cm^2)

Temperature differentials : Coefficient of thermal expansion = 0.000006 (1/°F)

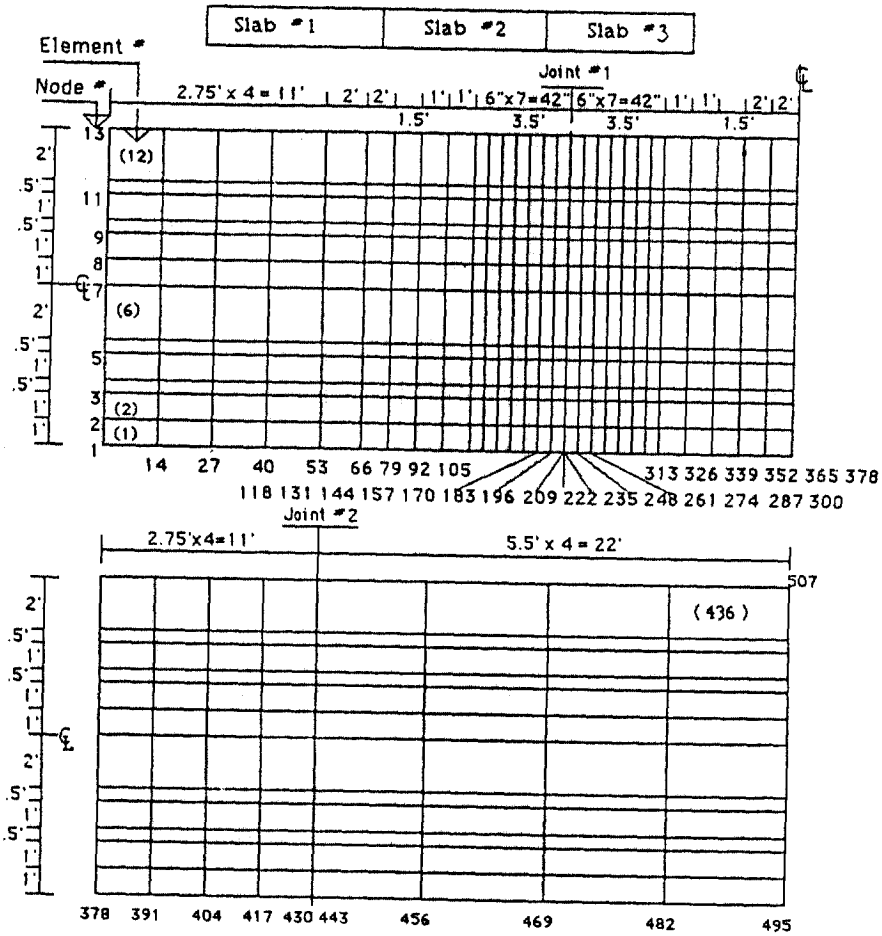

Fig. 5. Input Meshes for Joint Loadings

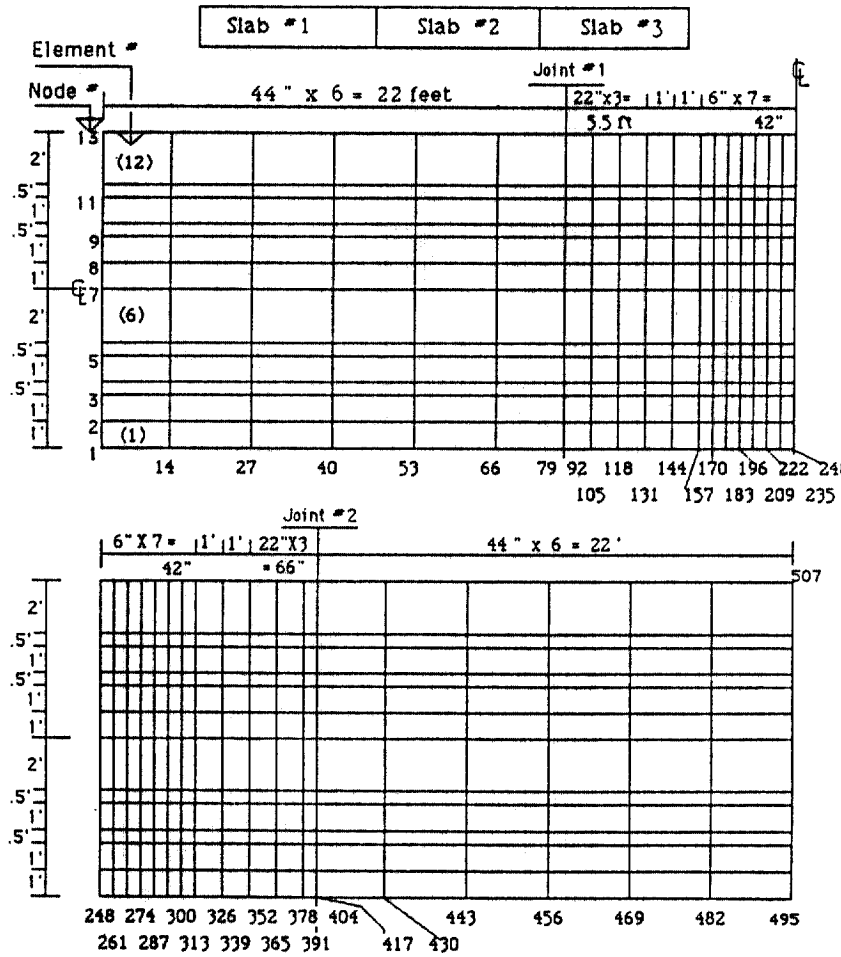

Fig. 6. Input Meshes for Mid-Slab Loading

Temperature differentials(=top-bottom)=0 ℉, −10 ℉(at night), +20 ℉ (day time)

Magnitude of axle load : AASHTO HS20-32 kips per axle. Maximum possible load =32×1.25=40 kips (18.16 ton) per axle.

Input meshes : Refer to Figure 5 and 6

5. 2. Results : Effects of skewed joint

The maximum stress in the slab caused by a 40 kip (18.16 ton) single axle load(which is two 20 kip (9.08 ton) wheel load at 6 feet (1.8 m) apart) applied at a skewed joint was computed and compared to that caused by the same 40 kip(18.16 ton) axle load at a regular transverse joint.

(1) Joint Edge Loading

The maximum flexural stress caused by a 40 kip joint edge load and a+20 ℉ temperature differential was computed with skewed angles A=0, 9.4, 18.4 ° and are tabulated in Table 1.

The maximum computed bending and shear stress at the regular transverse joint(A=90°) with $dT=+20$ ℉ temperature differential were a longitudinal tensile stress of $\sigma_x=598$ psi (41.9 kg/cm^2) at the top surface of the slab and just to the right of the joint (Node

Table 1. Effelcts of Skewed Joints on Maximum Stresses due to a Joint Edge 40 KIPS Axle Loading

Skew Angel	maximum stress (psi)			maximum principal stress (psi)		
	σ_{xx}	σ_{yy}	σ_{xy}	σ_1	σ_2	σ_{max}
A=0	598.3 (242N)	678.3 (229N)	93.4 (270N)	678.9 (229N)	594.7 (242N)	250.5 (209N)
A=9.46	607.3 (203N)	743.1 (216N)	105.4 (507N)	754.2 (216N)	594.9 (203N)	293.8 (222N)
A=18.4	665.1 (177N)	628.2 (177N)	127.0 (507F)	678.9 (177N)	608.4 (177N)	438.1 (209N)

Input data : Ks = 0.175 ksi, dT = +20 °F(* 1 ksi=70 kg/cm²)
Ke = 10 ksi, $K1$ = 10 ksi, Kr=16,000 k

* The numbers in parenthese denote node numbers at which maximum stress occrs. N denotes near the loading zone and F denotes far away from the loading zone.

number 242), and a transverse tensile stress of σ_y=678 psi(47.5 kg/cm²), located near the center line along the joint, and a shear stress of σ_{xy}=93 psi(6.5 kg/cm²), located very near the loading point.

A similar analysis was done with a skew angle of 9.46°, but using the same slab length and input parameters. The maximum computed bending and shear stresses were a longitudinal tensile stress of σ_x=608 psi(42.6 kg/cm²), located near the joint, a transverse tensile stress of σ_y=743 psi(52 kg/cm²) and a shear stress of σ_{xy}=105 psi(7.4 kg/cm²).

Referring to Table 1, which gives results for joint edge loading, the major principal stress, σ_1 increases and then decrease with increased skew angle. The minor principal stress increases, but only for the highest skew angle, while the shear stresses increases continually. In no case, however, are the variations in stress truly striking.

Another way of evaluating the effect of skewed joints on concrete pavement is through a maximum principal stress profile, showing lines of constant principal stress on the surface of the slab. This provides a very concise way of looking at the distribution of stresses, and will be used throughout this chapter. Figure 7 shows the effects of skewed joints on the maximum principal stress pro-

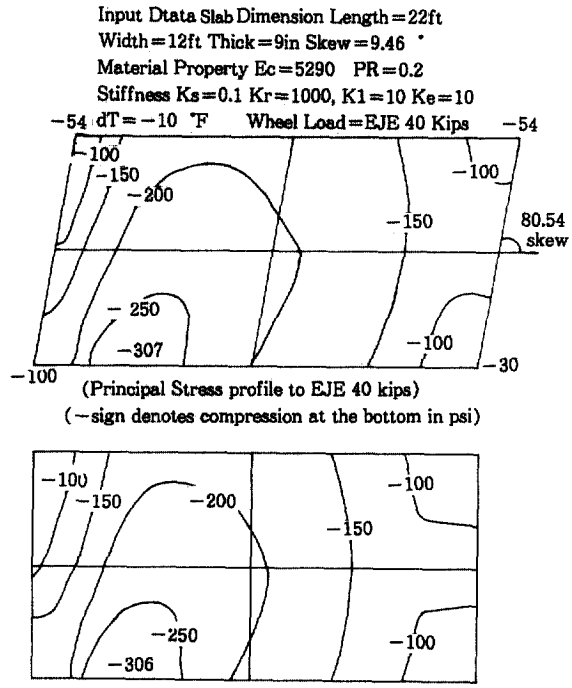

Fig. 7. Effects of Skewed Joint on Principal Stress Profile.

file associated with an equivalent joint edge load of 40 kips and a −10 °F temperature differential. It is seen that even though the variations in maximum stress displayed in Table 1 are not drastic, these higher stress levels are reached closer to the corner when the joint is skewed. This may well have a more powerful effect on behavior, even though there are small changes in maximum

Table 2. Effelcts of Skewed Joints on Maximum Stresses due to a Mid-Slab Loading of 40 KIPS.

Skew Angel	maximum stress (σ_{xx})	(σ_{yy})	(σ_{xy})	maximum principal stress (σ_1)	(σ_2)	(σ_{max})
A=0	744.3 (249N)	564.9 (255N)	77.6 (507N)	744.3 (249N)	564.9 (255N)	337.6 (248N)
A=9.46	747.8 (275N)	575.7 (255N)	101.7 (507N)	748.0 (275N)	575.4 (255N)	335.9 (274N)
A=18.4	579.6 (275N)	603.2 (229N)	120.4 (505F)	760.3 (275N)	601.7 (229N)	353.9 (287N)

Input data : Ks = 0.175 ksi, dT = +20 ℉(* 1 ksi=70 kg/cm²)
Ke = 10 ksi, $K1$ = 10 ksi, Kr=16,000 k

* The numbers in parentheses denote node numbers at which maximum stress occrs. N denotes near the loading zone and F denotes far away from the loading zone.

stress.

(2) Mid-Slab Edge Loading

Second, the maximum stresses in the slab caused by the combination of a 40 kip single axle load at the mid slab edge and a temperature differential of +20 ℉ in the slab were computed for both skewed and perpendicular joint and the results are shown in Table 2.

Table 2 shows that with an equivalent mid-slab edge load of 40 kips and +20℉ temperature differential, the maximum flexural and principal stresses are slightly increasing as the skew angle grows. Therefore, it can be concluded that the use of a skewed joints in concrete pavements induces slightly higher stresses, which should not in themselves affect structural performance. However, the higher stress are attained closer to the corner, which may or may not affect structural performance significantly.

(3) Stress Investigations For The Corner Crack Problems With Skewed Joint

One aspect of the deterioration of the I-75 skewed joint concrete pavement is corner cracking, which occurs mostly at the acute corner of a slab. It was decided to supplement the conclusions of the stress levels very close to the corner. The results of these analyses are shown in Table 3.

Table 3. Stress Investigation at the Joint Edge corner.

Input Parameter:Slab L=22ft, W=12ft, T=9in
Concerte Ec=5290, Joint Load=40 Kip
Stiffness Ks=0.175. Ke=10, K1=10, Kr=16000
Zero Temperature Differential case.

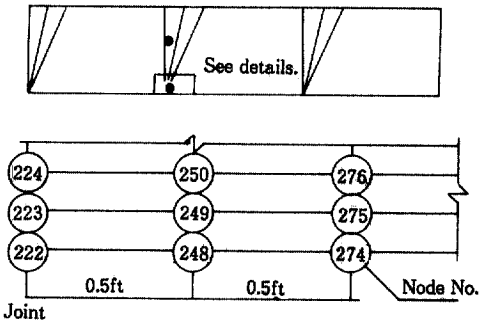

	Skew Angle	Node No. 222 223 224 248 249 250 274 275 276
σ_x psi	0	249 249 203 207 210 178 −16 10 36
	9.46	220 246 201 237 210 151 8 13 18
	18.46	160 241 192 235 206 120 11 11 −0.2
σy psi	0	47 224 92 34 160 77 1 73 45
	9.46	--52 253 186 −2.2188 128 −33 95 74
	18.46	−316 227 217 −118 200 142 −144 110 79

As expected, Table 3 shows that flexural stress in the X-direction due to the 40 kip joint edge load decreases very slightly as skew angle grows. However, the flexural stress in the Y-direction increases as skew angle increases significantly for the higher skew angles. This result, coupled with the presence of higher principal stresses closer

to the joint, may contribute to the higher frequency of corner cracking on the skewed joint pavement.

6. Conclusions

Skewed angle 9.46° and 18.46° in the concrete pavement were analyzed and compared to those of normal joint pavement to evaluate the structural performance of skewed joint concrete pavement.

The main conclusions of this research are summarized as follows : the maximum principal stress of skewed joint pavement is slightly higher than that of normal joint pavement, about 0 to 10 % depending on the subgrade modulus, temperature differentials, and live load positions. Furthermore stress concentrations on the acute joint are observed to be a possible cause of corner cracking failures. Therefore, it can be concluded that the use of skewed joint in concrete pavement may not be beneficial to the structural performance of pavement system.

Obviously, use of higher order displacement function and a large number of nodal meshes will lead to better accuracy. Our 12 degrees of freedom plate bending element, called MZC rectangle developed by Melosh, Zienkiewicz, and Chung[5], is nonconforming because normal slopes are not compatible, and discontinuities occur at adjoining edges. Subsequently, use of BFS rectangle, developed by Bogner, Fox, and Schmit[5], generally produces greater accuracy than the MZC rectangle because of a higher order displacement function (16 degrees of freedom) and and a larger number of nodal displacements. Nevertheless, both MZC and BFX rectangle can model states of constant strain for a flexture in plate, and they also have complete and balanced displacement funciton, which produces great convergence.

References

1. Jo, Byung-wan, "*A Finite Element Parametric Study for the Response of Concrete Higyway Pavements with Skewed Joints*", Doctoral thesis, Department of Civil Engineering, University of Florida, 1988.
2. Tia, Mang, Armaghani, J. M., "*Field Evaluation of Rigid Pavements for the Development of a Rigid Pavement Design System-Phase I*", University of Florida Final Report, 1986.
3. Lei, Shau, "*Analysis of Three Slabs Concrete Pavement Systems Using Finite Element Analysis Method*", Masters Thesis, Department of Civil Engineering, University of Florida, 1985.
4. Kevin, L. Toy, "*Analysis of Rigid Concrete Pavements*", Master Thesis, Department of Civil Engineering, University of Florida, 1984.
5. Zienkiewicz, O. C. "*Finite Elements for Structural and Continuum Mechanics, 3rd edition,*" London, McGraw-hill, 1977.
6. Timoshenko and Woinowsky-Krieger, "*Theory of Plates and Shells, 2 nd Edition*", McGraw-hill, 1959.
7. "*AASHTO Guide for Design of Pavement Structures,*" American Association of State Highway and Transportation Officials, 1986.

(接受 : 1988. 11. 10)

APPENDIX : STIFFNESS MATRIX OF PARALLELOGRAMMIC PLATE BENDING ELEMENT (12×12 SYMMETRIC)

$A_4+C_1C_1+C_2C_2+1.9C_3C_3$ $+PR(2C_1+0.5C_2)$ $+D_{xy}(4H_{44}+\frac{7}{5}H_{55})$			
$-0.7C_1C_7-C_2C_7$ $-PR(0.5C_7)$ $-0.2\,D_{xy}\,H_{58}$	$\frac{8}{15}C_6C_6+\frac{4}{3}C_7C_7-C_6C_7$ $+D_{xy}(\frac{8}{15}P_{88})$		
$A_3+C_1C_9+0.7C_2C_9$ $+PR(2C_1D+0.5C_2D)$ $+D_{xy}(4C_1D+0.2C_2D)$	$\frac{1}{6}C_6C_9-C_7C_9+PR(\frac{1}{6}DC_6$ $-DC_7)+DXY\frac{1}{3}P_{81}$	$\frac{4}{3}A_2+\frac{4}{3}C_9C_9-\frac{7}{15}C_{10}C_{10}$ $+\frac{1}{3}C_9C_{10}+PR\frac{8}{3}(Z_4-Z_5)$ $+DXY(\frac{16}{3}Q_{11}+\frac{8}{15}Q_{22}-2Q_{12})$	
$0.5A_4+0.5C_1C_1-C_2C_2$ $-1.9C_3C_3+PR(C_1-0.5C_2)$ $+DXY(2H_{44}-\frac{7}{5}H_{55})$	$0.2C_1C_7+C_2C_7$ $+DXY(0.2H_{58})$	$0.5A_3+0.5C_1C_9-C_1C_{10}$ $-0.7C_2C_9+PR(C_1D-C_3D$ $-0.5C_2D)+DXY(2C_1D$ $-2C_3D-0.2C_2D)$	$A_4+C_1C_1+C_2C_2+1.9C_3C_3$ $+PR(2C_1+0.5C_2)$ $+DXY(4H_{44}+\frac{7}{5}H_{55})$
$-0.2C_1C_7-C_2C_7$ $+DXY(-0.2H_{58})$	$-\frac{2}{15}C_6C_6+\frac{2}{3}C_7C_7$ $+DXY(-\frac{2}{15})P_{88}$	$-\frac{1}{6}C_6C_9+PR(-\frac{1}{6})DC_6$ $+DXY(-\frac{1}{3})P_{81}$	$0.7C_1C_7+C_2C_7$ $+PR0.5C_7+DXY0.2H_{58}$
$0.5A_3+0.5C_1C_9+C_1C_{10}$ $-0.7C_2C_9+PR(C_1D-0.5C_2D$ $+C_3D)+DXY(2C_1D+2C_3D$ $-0.2C_2D)$	$-\frac{1}{6}C_6C_9+PR(-\frac{1}{6})DC_6$ $+DXY(-\frac{1}{3})P_{81}$	$\frac{2}{3}A_2+\frac{2}{3}C_9C_9-\frac{8}{15}C_{10}C_{10}$ $+PR\frac{4}{3}Z_4+DXY(\frac{8}{3}Q_{11}$ $-\frac{8}{15}Q_{22})$	$A_3+C_1C_9+0.7C_2C_9$ $+PR(2C_1D+0.5C_2D)$ $+DXY(4C_1D+0.2C_2D)$
$-A_4-C_1C_1+0.5C_2C_2$ $-1.9C_3C_3+PR(-2C_1-0.5C_2)$ $+DXY(-4H_{44}-\frac{7}{5}H_{55})$	$0.7C_1C_7+C_2C_6-0.5C_2C_7$ $+PR0.5C_7+DXY0.2H_{58}$	$-A_3-C_1C_9-0.2C_2C_9$ $+PR(-2C_1D)$ $+DXY(-4C_1D-0.2C_2D)$	$-0.5A_4-0.5C_1C_1-0.5C_2C_2$ $+1.9C_3C_3+PR(-C_1+0.5C_2)$ $+DXY(-2H_{44}+\frac{7}{5}H_{55})$
$0.7C_1C_7-C_2C_6-0.5C_2C_7$ $+PR0.5C_7+DXY0.2H_{58}$	$-\frac{8}{15}C_6C_6+\frac{2}{3}C_7C_7$ $+DXY(-\frac{8}{15})P_{88}$	$-\frac{1}{6}C_6C_9+PR(-\frac{1}{6})DC_6$ $+DXY(-\frac{1}{3})P_{81}$	$-0.2C_1C_7+C_2C_6+0.5C_2C_7$ $+DXY(-0.2)H_{58}$
$A_3+C_1C_9+0.2C_2C_9$ $+PR2C_1D+DXY(4C_1D$ $+0.2\,C_2D)$	$-\frac{1}{6}C_6C_9+PR(-\frac{1}{6})DC_6$ $+DXY(-\frac{1}{3})P_{81}$	$\frac{2}{3}A_2+\frac{2}{3}C_9C_9-\frac{2}{15}C_{10}C_{10}$ $+PR\frac{4}{3}Z_4+DXY(\frac{8}{3}Q_{11}$ $-\frac{2}{15}Q_{22})$	$0.5A_3+0.5C_1C_9+C_1C_{10}$ $-0.2C_2C_9+PR(C_1D+C_3D)$ $+DXY(2C_1D+2C_3D$ $-0.2C_2D)$
$-0.5A_4-0.5C_1C_1-0.5C_2C_2$ $+1.9C_3C_3+PR(-C_1+0.5C_2)$ $+DXY(-2H_{44}+\frac{7}{5}H_{55})$	$-0.2C_1C_7-C_2C_6+0.5C_2C_7$ $+DXY(-0.2H_{58})$	$-0.5A_3-0.5C_1C_9+C_1C_{10}$ $+0.2C_2C_9+PR(-C_1D$ $+C_3D)+DXY(-2C_1D$ $+2C_3D+0.2C_2D)$	$-A_4-C_1C_1+0.5C_2C_2$ $-1.9C_3C_3+PR(-2C_1-0.5C_2)$ $+DXY(-4H_{44}-\frac{7}{5}H_{55})$
$0.2C_1C_7+C_2C_6-0.5C_2C_7$ $+DXY0.2H_{58}$	$\frac{2}{15}C_6C_6+\frac{1}{3}C_7C_7-C_6C_7$ $+DXY\frac{2}{15}P_{88}$	$\frac{1}{6}C_6C_9+PR\frac{1}{6}DC_6$ $+DXY\frac{1}{3}P_{81}$	$-0.7C_1C_7-C_2C_6+0.5C_2C_7$ $+PR(-0.5C_7)$ $+DXY(-0.2H_{58})$
$0.5A_3+0.5C_1C_9-C_1C_{10}$ $-0.2C_2C_9+PR(C_1D-C_3D)$ $+DXY(2C_1D-2C_3D-0.2C_2D)$	$\frac{1}{6}C_6C_9+PR\frac{1}{6}DC_6$ $+DXY\frac{1}{3}P_{81}$	$\frac{1}{3}A_2+\frac{1}{3}C_9C_9+\frac{2}{15}C_{10}C_{10}$ $-C_9C_{10}+PR(\frac{2}{3}Z_4-Z_5)$ $+DXY(\frac{4}{3}Q_{11}+\frac{2}{15}Q_{22}-2Q_{12})$	$A_3+C_1C_9+0.2C_2C_9$ $+PR2C_1D$ $+DXY(4C_1D+0.2C_2D)$

Natations :

$A_1=1/A$ $B_1=1/B$

$A_2=1/A^2$ $B_2=1/B^2$

$A_3=1/A^3$ $B_3=1/B^3$

$A_4=1/A^4$ $B_4=1/B^4$

$C_2C_7=B_3\cdot\mathrm{cosec}^4(\alpha)$

$C_6C_9=A_2\cdot\cot^3(\alpha)\cdot\mathrm{cosec}(\alpha)$

$C_7C_9=A_1\cdot B_1\cdot\cot^2(\alpha)\cdot\mathrm{cosec}^2(\alpha)$

$C_9C_9=A_2\cdot\cot^4(\alpha)$

$\frac{8}{15}C_6C_6+\frac{4}{3}C_7C_7+C_6C_7$ $+DXY\frac{8}{15}P_{88}$			
$\frac{1}{6}C_6C_9+C_7C_9+PR(\frac{1}{6}DC_6$ $+DC_7)+DXY\frac{1}{3}P_{81}$	$\frac{4}{3}A_2+\frac{4}{3}C_9C_9+\frac{8}{15}C_{10}C_{10}$ $+C_9D_{10}+PR(\frac{8}{3}Z_4+Z_5)$ $+DXY(\frac{16}{3}Q_{11}+\frac{8}{15}Q_{22}+2Q_{12})$		
$0.2C_1C_7-C_2C_6-0.5C_2C_7$ $+DXY0.2H_{58}$	$-0.5A_3-0.5C_1C_9-C_1C_{10}$ $+0.2C_2C_9+PR(-C_1D-C_3D)$ $+DXY(-2C_1D-2C_3D)$ $+0.2C_2D)$	$A_4+(C_1C_1+C_2C_2+1.9C_3C_3$ $+PR(2C_1+0.5C_2)$ $+DXY(4H_{44}+\frac{7}{5}H_{55})$	
$\frac{2}{15}C_6C_6+\frac{1}{3}C_7C_7+C_6C_7$ $+DXY\frac{2}{15}P_{88}$	$\frac{1}{6}C_6C_9+PR\frac{1}{6}DC_6$ $+DXY\frac{1}{3}P_{81}$	$-0.7C_1C_7-C_2C_7$ $+PR(-0.5C_7)$ $+DXY(-0.2H_{58})$	$\frac{8}{15}C_6C_6+\frac{4}{3}C_7C_7+C_6C_7$ $+DXY\frac{8}{15}P_{88}$
$\frac{1}{6}C_6C_9+PR\frac{1}{6}DC_6$ $+DXY\frac{1}{3}P_{81}$	$\frac{1}{3}A_2+\frac{1}{3}C_9C_9+\frac{2}{15}C_{10}C_{10}$ $+C_9C_{10}+PR(\frac{2}{3}Z_4+Z_5)$ $+DXY(\frac{4}{3}Q_{11}+\frac{2}{15}Q_{22}+2Q_{12})$	$-A_3-C_1C_9-0.7C_2C_9$ $+PR(-2C_1D-0.5C_2D)$ $+DXY(-4C_1D-0.2C_2D)$	$\frac{1}{6}C_6C_9+C_7C_9$ $+PR(\frac{1}{6}DC_6+DC_7)$ $+DXY\frac{1}{3}P_{81}$
$-0.7C_1C_7+C_2C_6+0.5C_2C_7$ $+PR(-0.5C_7)$ $+DXY(-0.2H_{58})$	$-A_3-C_1C_9-0.2C_2C_9$ $+PR(-2C_1D)$ $+DXY(-4C_1D-0.2C_2D)$	$0.5A_4+0.5C_1C_1-C_2C_2$ $-1.9C_3C_3+PR(C_1-0.5C_2)$ $+DXY(2H_{44}-\frac{7}{5}H_{55})$	$0.2C_1C_7+C_2C_7$ $+DXY0.2H_{58}$
$-\frac{8}{15}C_6C_6+\frac{2}{3}C_7C_7$ $+DXY(-\frac{8}{15})P_{88}$	$-\frac{1}{6}C_6C_9+PR(-\frac{1}{6})DC_6$ $+DXY(-\frac{1}{3})P_{81}$	$-0.2C_1C_7-C_2C_7$ $+DXY(-0.2H_{58})$	$-\frac{2}{15}C_6C_6+\frac{2}{3}C_7C_7$ $+DXY(-\frac{2}{15})P_{88}$
$-\frac{1}{6}C_6C_9+PR(-\frac{1}{6})DC_6$ $+DXY(-\frac{1}{3})P_{81}$	$\frac{2}{3}A_2+-\frac{2}{3}C_9C_9-\frac{2}{15}C_{10}C_{10}$ $+PR\frac{4}{3}Z_4$ $+DXY(\frac{8}{3}Q_{11}-\frac{2}{15}Q_{22})$	$-0.5A_3-0.5C_1C_9+C_1C_{10}$ $+0.7C_2C_9+PR(-C_1D$ $+0.5C_2D+C_3D)+DXY$ $(-2C_1D+2C_3D+0.2C_2D)$	$-\frac{1}{6}C_6C_9+PR(-\frac{1}{6})DC_6$ $+DXY(-\frac{1}{3})P_{81}$

· *Element stiffness matrix*

$$SK(i,\ j)\ i=1,\ 12\ = a\,b\ \sin(\alpha)\ [SK_1 \cdot D_x + SK_2 \cdot D_y + SK_3 \cdot D_1 + SK_4 \cdot D_{xy}]$$
$$j=1,\ 12$$

For isotrofic material

$D_x = D_y = 1$

$D_1 = PR$(Poisson's Ratio)

$D_{xy} = (-PR)/2$

$C_1C_1 = A_4 \cdot \cot^4(\alpha)$

$C_2C_2 = B_4 \cdot \mathrm{cosec}^4(\alpha)$

$C_3C_3 = A_2 \cdot B_2 \cdot \cot^2(\alpha),\ \mathrm{cosec}^2(\alpha)$

$C_6C_6 = A_2 \cdot \cot^2(\alpha) \cdot \mathrm{cosec}^2(\alpha)$

$C_{10}C_{10} = B_2 \cdot \cot^2(\alpha) \cdot \mathrm{cosec}^2(\alpha)$

$C_9C_{10} = A_1 \cdot B_1 \cot^3(\alpha) \cdot \mathrm{cosec}(\alpha)$

$C_1C_9 = A_3 \cdot \cot^4(\alpha)$

$C_1C_{10} = A_2 \cdot B_1 \cdot \cot^3(\alpha) \cdot \mathrm{cosec}(\alpha)$

$C_7 = A_2 \cdot B_1 \cdot \mathrm{cosec}^2(\alpha)$

$C_1D = A_3 \cdot \cot^2(\alpha)$

$C_2D = A_1 \cdot B_2 \cdot \mathrm{cosec}^2(\alpha)$

$C_3D = A_2 \cdot B_1 \cdot \cot(\alpha) \cdot \mathrm{cosec}(\alpha)$

$C_7C_7 = B_2 \cdot \mathrm{cosec}^4(\alpha)$

$C_6C_7 = A_1 \cdot B_1\ \cot(\alpha) \cdot \mathrm{cosec}^3(\alpha)$

$C_1C_7 = A_2 \cdot B_1\ \cot^2(\alpha) \cdot \mathrm{cosec}^2(\alpha)$

$C_2C_6 = A_1 \cdot B_2\ \cot(\alpha) \cdot \mathrm{cosec}^3(\alpha)$

$C_2C_9 = A_1 \cdot B_2\ \cot^2(\alpha) \cdot \mathrm{cosec}^3(\alpha)$

$C_2C_{10} = B_3 \cdot \cot(\alpha) \cdot \mathrm{cosec}^3(\alpha)$

$C_1 = A_4 \cdot \cot^2(\alpha)$

$C_2 = A_2 \cdot B_2 \cdot \mathrm{cosec}^2(\alpha)$

$DC_6 = A_2 \cdot \cot(\alpha) \cdot \mathrm{cosec}(\alpha)$

$DC_7 = A_1 \cdot B_1 \cdot \mathrm{cosec}^2(\alpha)$

$Z_4 = A_2 \cdot \cot^2(\alpha)$

$Z_5 = A_1 \cdot B_1 \cdot \cot(\alpha) \cdot \mathrm{cosec}(\alpha)$

$H_{44} = A_4 \cdot \cot_2(\alpha)$

$H_{55} = A_2 \cdot B_2 \cdot \mathrm{cosec}^2(\alpha)$

$H_{45} = A_3 \cdot B_1 \cdot \cot(\alpha) \cdot \mathrm{cosec}(\alpha)$

$H_{48} = A_3 \cdot \cot(\alpha) \cdot \mathrm{cosec}(\alpha)$

$H_{58} = A_2 \cdot B_1 \cdot \mathrm{cosec}^2(\alpha)$

$P_{88} = A_2 \cdot \mathrm{cosec}^2(\alpha)$

$P_{81} = A_2 \cdot \cot(\alpha) \cdot \mathrm{cosec}(\alpha)$

$P_{82} = A_1 \cdot B_1\ \mathrm{cosec}^2(\alpha)$

$Q_{11} = A_2 \cdot \cot^2(\alpha)$

$Q_{22} = B_2 \cdot \mathrm{cosec}^2(\alpha)$

$Q_{12} = A_1 \cdot B_1 \cdot \cot(\alpha)\ \mathrm{cosec}(\alpha)$

$\frac{4}{3}A_2+\frac{4}{3}C_9C_9+\frac{8}{15}C_{10}C_{10}$ $+C_9C_{10}+PR(\frac{8}{3}Z_4+Z_5)$ $+DXY(\frac{16}{3}Q_{11}+\frac{8}{15}Q_{22}+2Q_{12})$			
$-0.5A_3-0.5C_1C_9-C_1C_{10}$ $+0.7C_2C_9+PR(-C_1D-C_3D$ $+.5C_2D)+DXY(-2C_1D$ $-2C_3D+0.2C_2D)$	$A_4+C_1C_1+C_2C_2+1.9C_3C_3$ $+PR(2C_1+0.5C_2)$ $+DXY(4H_{44}+\frac{7}{5}H_{55})$		
$-\frac{1}{6}C_6C_9+PR(-\frac{1}{6})DC_6$ $+DXY(-\frac{1}{3})P_{81}$	$0.7C_1C_7+C_2C_7$ $+PR0.5C_7+DXY0.2H_{58}$	$\frac{8}{15}C_6C_6+\frac{4}{3}C_7C_7-C_6C_7$ $+DXY\frac{8}{15}P_{88}$	
$\frac{2}{3}A_2+\frac{2}{3}C_9C_9-\frac{8}{15}C_{10}C_{10}$ $+PR\frac{4}{3}Z_4+DXY(\frac{8}{3}Q_{11}$ $-\frac{8}{15}Q_{22})$	$-A_3-C_1C_9-0.7C_2C_9$ $+PR(-2C_1D-0.5C_2D)$ $+DXY(-4C_1D-0.2C_2D)$	$\frac{1}{6}C_6C_9-C_7C_9$ $+PR(\frac{1}{6}DC_6-DC_7)$ $+DXY\ \frac{1}{3}P_{81}$	$\frac{4}{3}A_2+\frac{1}{3}C_9C_9-\frac{7}{15}C_9C_{10}$ $+PR(\frac{8}{3}Z_4-Z_5)$ $+DXY(\frac{16}{3}Q_{11}+\frac{8}{15}Q_{22}-2Q_{12})$